Functional Materials 12, No.2 (2005) © 2005 — Institute for Single Crystals

Dopant concentration dependence of thermostimulated luminescence in $Li_2B_4O_7$:Mn single crystals

V.M.Holovey, V.I.Lyamayev, M.M.Birov, P.P.Puga, A.M.Solomon

Institute of Electron Physics, National Academy of Sciences of Ukraine,
21 Universitetska St., 88000 Uzhgorod, Ukraine

A series of $Li_2B_4O_7$:Mn single crystals with different dopant concentrations has been produced and their thermoluminescence (TL) has been studied. The glow curve shapes differ significantly with increase of Mn concentration, but all of them reveal two broad complex peaks. The results of fractional glow technique application show the presence of two groups, each with a large number of traps with close depths. Dose dependence of glow curves shape testifies to the first order of TL kinetics.

Получена серия монокристаллов $Li_2B_4O_7$:Mn с разной концентрацией легирующей примеси и исследована их термостимулированная люминесценция (ТСЛ). Форма кривых термовысвечивания (КТВ) существенно изменяется при повышении концентрации Mn, но на всех них можно выделить два сложных максимума. Результаты применения метода частичного высвечивания светосуммы указывают на наличие двух групп ловушек, каждая из которых содержит несколько уровней прилипания с близкими величинами энергии активации. Зависимость формы КТВ от поглощенной дозы свидетельствует о первом порядке кинетики ТСЛ.

Crystalline manganese-doped lithium tetraborate (LTB) $Li_2B_4O_7$:Mn is one of the known thermoluminescent crystal luminophors for X-ray and gamma dosimetry. Improvement of thermoluminophor characteristics, in particular, reduction of background signal, enhancement of light output due to collection of luminescent emission from the entire detector volume as well as reduction of hygroscopicity could be provided by using the single crystal samples [1]. Therefore, the manufacturing methods of doped (in particular, manganese-doped) LTB single crystals are being developed and their thermoluminescence (TL) properties are being studied [2]. We have obtained LTB:Mn single crystals with different dopant concentrations, studied their decay curves and determined the trap depths and TL kinetics order.

The initial blend for single crystal growing was prepared using extra-pure reagents by melting the stoichiometric amounts of B_2O_3 and Li_2CO_3 and calculated amount of MnO_2 in a platinum crucible in the air. Taking into account the incongruent character of LTB evaporation [3, 4], and in order to reduce the boron oxide loss during the single crystal growing, excess B_2O_3 (up to 0.3 mol.%) was added to the blend. The single crystals were grown by Czochralski method along the <100> direction at the 3 mm/day pulling rate and 5–10 rpm rotation speed. In the lower part of single crystals produced, the solid phase and gas inclusions were observed. With increasing dopant content in the initial blend, the size of areas free of macrodefects in the upper part of single crystals decreased. A certain amount of gas inclusions was also observed along the single crystal growth axis. This could be explained by insufficient melt mixing in the central part of sub-crystal region due to its high viscosity [5, 6]. In general, distribution of inclusions in the crystal bulk was similar to that reported in [7], where the most defect areas were located in the central part of single crystals along the

growth axis and formed a circular areas, while their number was much less close to the outer surface. With increasing manganese content in the initial blend, the size of crystal areas with solid phase and gas inclusions also increased. The X-ray analysis results of high-quality LTB:Mn crystal parts are almost similar to the literature data obtained for undoped LTB single crystals [8] and show the absence of other phases — borates and manganese oxides (within the sensitivity limits of the method). Samples for the studies were cut out from the crystal parts free of macrodefects normally to the pulling direction. The measurements were carried out at polished samples of $6\times6\times1$ mm^3 size.

To determine the concentration dependence of TL yield in LTB:Mn single crystals, we have performed a series of similar annealing/irradiation/measurement cycles for the samples with different dopant concentrations. The annealing was done at 400°C for 100 s. The samples were irradiated using an X-ray tube with copper anti-cathode at 20 kV operating voltage. The absorbed dose was 2 Gy at 2 Gy/min dose rate. The decay curves were recorded immediately after exposure using an automated setup equipped with a FEU-136 photomultiplier operating in the photon counting mode. To minimize the effect of sample and heater thermal emission, a SZS-24 light filter was mounted in front of the photomultiplier window. The linear heating rate of the sample was 0.5°C/s. A thin layer of silicon grease was introduced between the heater and sample to improve the thermal contact. For each dopant concentration, the experiment was repeated using several samples cut out of the same part of the single crystal. The data obtained were averaged, and the measurement error was determined by a standard procedure.

The fractional glow technique (FGT) was applied to investigate the trap parameters. The pre-annealed samples were exposed to X-ray dose of about 100 Gy. During each FGT cycle, the sample temperature was repeatedly increased by 7°C at about 0.1°C/s rate and lowered by 5°C at the same rate. The above parameters appeared to be optimal from the standpoint of the method resolution and measuring time. The whole procedure consisted of about 100 heating/cooling cycles. The average depth value E_i of all traps emptied in the i-th cycle was calculated using the formula proposed in [9]

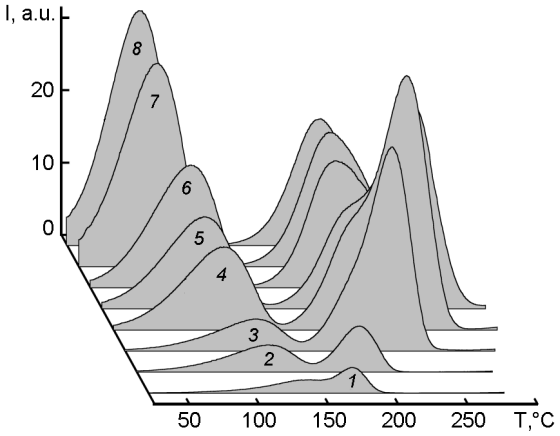

Fig. 1. Glow curves of $Li_2B_4O_7$:Mn single crystal samples with different Mn concentration in the initial blend (mass.%): 0.001 (*1*), 0.002 (*2*), 0.006 (*3*), 0.016 (*4*), 0.024 (*5*), 0.033 (*6*), 0.1 (*7*), 0.16 (*8*).

and taking into account the difference between the heating and cooling ratio in a cycle:

$$E_i = E_{ih} + \frac{w_{ic}}{w_{ih} + w_{ic}}(E_{ic} - E_{ih}), \qquad (1)$$

where E_{ih} and E_{ic} are, the energies estimated for the heating and cooling part of TL curve, respectively, in i-th cycle; w_{ih} and w_{ic}, the linear heating and cooling rates in the i-th cycle, respectively.

The luminescence emission of the single crystal (as well as crystalline) LTB:Mn is in the orange region of the visible spectrum. Fig. 1 shows glow curves of LTB:Mn single crystal samples with different Mn concentration in the initial blend. As is seen, the curves shape changes significantly as the dopant concentration varies, but all the curves demonstrate two well separated broad peaks, the first lying within the 25–150°C range and second, within the 150–280°C one. The peak shapes correlate with the data of [10] obtained for the crystalline samples but differs from those for the single crystal ones [2]. As the dopant concentration increases, the intensity of the low-temperature peak rises, thus exceeding that of the high-temperature one, while its position shifts towards lower temperatures. The concentration dependence for the high-temperature peak has a more complex character. Namely, as the dopant concentration increases, it is first broadened towards higher temperatures with simultaneous intensity rise and attains a maximum. At fur-

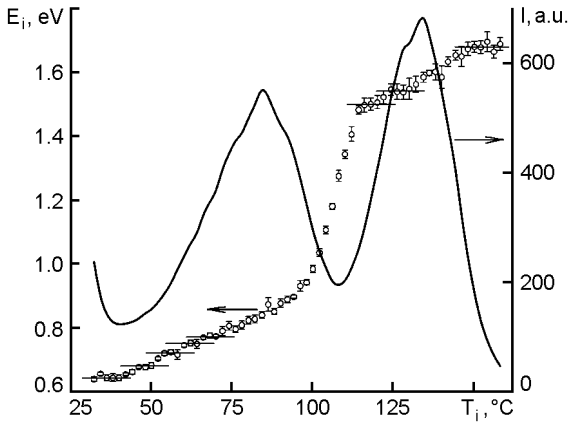

Fig. 2. The FGT results for $Li_2B_4O_7$:Mn single crystal sample with 0.001 mass.% Mn concentration in the initial blend.

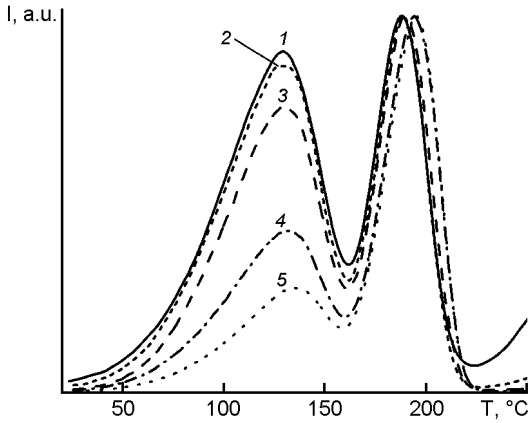

Fig. 3. Glow curves of $Li_2B_4O_7$:Mn single crystal sample with 0.002 mass.% Mn concentration in the initial blend irradiated with different doses (Gy): 0.035 (*1*), 0.14 (*2*), 0.56 (*3*), 3.6 (*4*), 14 (*5*).

ther increase of the dopant concentration, this peak first continues to broaden, slightly decreasing in amplitude, and then becomes narrower towards the lower temperatures keeping almost unchanged form.

Fig. 2 presents the results of the FGT measurement for one of the samples. The symbols present the obtained trap depth values, while the curve reflects the light sum emitted in each cycle. The abscissa corresponds to the maximum temperature in the cycle. In the left-hand part of this plot that corresponds to the group of traps responsible for the low-temperature complex TL peak, there is several more and less pronounced plateaus. This indicates the presence of several traps in the crystal with small difference in their depths. The above difference is close to the FGT resolution, which, according to [11], is 25 meV; that complicates the identification of these traps. The most pronounced plateaus correspond to energy values of 0.64, 0.68, 0.72, 0.75, and 0.77 eV. In the high-temperature part of Fig. 2, the error is much greater, nevertheless, some plateaus can be distinguished. This also indicates the presence of a group of traps with close depths, that are responsible for the high-temperature complex TL peak. The most pronounced plateaus correspond to energy values of 1.5, 1.54, and 1.68 eV.

The results of FGT application to the samples with other dopant concentrations also indicate the presence of two trap groups, each including a large number of traps with close depths. In addition, it has been found that the most of obtained energy values are common for most samples with different dopant concentration. This may testify to the similarity of the energy structure of the above single crystals. In that case, the change of the decay curve shape with varying dopant concentration could be explained by redistribution of the elementary peak intensities that form two complex peaks or, more clearly, by redistribution of traps filling during the irradiation of the sample.

To determine the order of the TL kinetics, we have studied the dependence of decay curve shape on the absorbed dose for several samples with different dopant concentration. Fig. 3 shows glow curves for one of the samples normalized to unity. The irradiation doses were 0.035, 0.14, 0.56, 3.6, and 14 Gy, the linear heating rate was 1°C/s. As is seen from the Figure, as the absorbed dose increases, the high-temperature peak exceeds the low-temperature one at almost constant half-widths, while the temperature position is shifted towards higher temperatures by only 5°C. This insignificant shift could be explained by redistribution of the elementary peak intensities towards the high-temperature components. The slight change in the half-width and temperature position of the TL peak while the absorbed dose increases by a factor of 400 testifies to the first order of TL kinetics. Similar results and conclusions were obtained for the samples with other dopant content.

According to [8, 12], LTB belongs to so-called carcass structures based on the rigid anion sublattice formed by the 3D boron-oxygen net. Its basic structural fragment is

$B_4O_9^{6-}$-group, where two boron atoms are in the triangular and two, in the tetrahedral coordination. These complexes are integrated by common oxygen atoms into spirals with symmetry axis along the <001> direction. The spirals, in turn, are also combined by common oxygen atoms, while lithium ions are located in the hollows between the spirals. Electron density peaks in the B–O bonds are shifted towards oxygen, i.e. the chemical binding in the anion sublattice is polar covalent, while that between the lithium ions and anion sublattice is ionic one. In the anion sublattice, there are channels oriented along the <001> crystallographic direction, where tetrahedral-coordinated lithium ions are located. Those are relatively weakly bound with anion sublattice, thus providing both ionic conduction realized due to the lithium ions according to the vacancy mechanisms and a considerable electric conduction anisotropy [13].

It is known [14] that the boron-oxygen tetrahedrons in the LTB structure are produced due to attachment of an additional oxygen atom produced due to interaction of lithium oxide Li_2O with boron oxide B_2O_3, and the cations are located close to BO_4 tetrahedrons, thus compensating the excessive negative charge distributed over the tetrahedron [15]. Thus, tetrahedral complex becomes a negatively charged point defect provided it is isolated from the lithium cation that compensates the charge. The above point defects could act as hole traps. Oxygen vacancies in the structure form additionally charged point defects (holes) capable of trapping electrons. In some cases, electron and hole traps could be associated with bridging and non-bridging oxygen bonds [14].

In the process of LTB single crystal growth from the melt with boron oxide excess, the single crystal may, according to [16], contain up to ~0.1 mol.% of excessive B_2O_3 that corresponds to the limit of the compound homogeneity domain. Obviously, in this case, a certain number of negatively charged cation vacancies is produced, and their charge is compensated by the increased number of triangular boron-oxygen complexes and thus by the increasing ratio between the boron-oxygen tetrahedrons and triangles in the anion sublattice (which is 2:2 in stoichiometric LTB) in favor of the latter. In this case, the chemical composition of LTB does not exceed the homogeneity domain. Thus, both electron and hole traps appear mainly at the defects related to the basic structural units of the lattice.

Taking into account the peculiarities of LTB structure, in particular, the anion sublattice rigidity, dopant introduction into sublattice is most probable with the production of substitution (i.e. lithium ion substitution) and establishment (in the interstitial sites located in the conduction channels) solid solutions. It is also to take into account the ion size and its charge state. According to [17, 18], manganese enters LTB in the octahedral coordination in the form of Mn^{2+}, and this should be explained by decomposition of thermally unstable MnO_2 during the synthesis at temperatures above 535°C with MnO formation. In this case, the excessive charge of Mn_{Li} is compensated most likely by the increasing number of cation vacancies and boron-oxygen triangles in the anion sublattice due to formation of oxygen vacancies in the sites of bridge oxygen atoms. For instance, the ratio of the "physical" ionic radii for manganese and lithium $r_{Mn^{++}}/r_{Li^{+}}$ at the octahedral manganese coordination and tetrahedron lithium one is 1.10/0.73 = 1.51 [19]. This quantity is larger than that for copper (1.01) but is less as compared to silver (1.56). In the case of LTB:Mn single crystal growth from the melt with low (0.3–0.5 mol.%) excess of B_2O_3, a certain number of cation vacancies could be formed, thus making easier the formation of both substitution solid solution where lithium ion positions are occupied by manganese, and, probably, of establishment solid solution, where the latter could occupy interstitial positions in the conduction channels. When manganese enters the interstitial sites, the excessive Mn_i charge could also be compensated due to the formation of vacancies in the cation sublattice. In accordance with the data [20] obtained when studying the LTB thermoelectric properties, lithium atoms occupy energetically non-equivalent positions. On this basis, the dopant atoms (manganese) that substitute lithium may be assumed to be also energetically non-equivalent. This could stimulate the presence of several traps and, respectively, the complex structure of TL curve.

References

1. A.I.Nepomnyaschikh, S.N.Mironenko, G.I.Afonin et al., *Atomnaya Energia*, **58**, 257 (1985).
2. Kang-Soo Park, *J. Cryst. Growth*, **249**, 483 (2003).
3. K.Tada, M.Tatsumi, Ya.Namikawa, Japan Pat. Appl. No.62-108800.
4. D.S.Robertson, I.M.Young, *J. Mater. Sci.*, **17**, 1729 (1982).

5. M.Adachi, T.Shiosaki, A.Kawabata, *Jap.J. Appl.Phys.*, **24**, Suppl.3, Pt.1, 72 (1985).
6. V.A.Nefedov, B.L.Zadneprovski, *Ann.Chim. Sci.Mat.*, **22**, 703 (1997).
7. T.P.Balakireva, V.V.Lebold, V.A.Nefedov et al., *Izv.AN SSSR.Neorgan.Mater.*, **25**, 524 (1989).
8. S.F.Radaev, L.A.Muradian, L.F.Malakhova et al., *Kristallografiya*, **34**, 1400, (1989).
9. A.Chruscinska, *J.Luminescence*, **62**, 115 (1994).
10. R.Abubakar, S.Uhtung, M.Oberhofer, *Radiat. Prot. Dosim.*, **33**, 95 (1990).
11. A.Chruscinska, H.L.Oczkowski, K.R.Przegietka, *Acta Physica Polonica*, **A 89**, 555 (1996).
12. Ya.V.Burak, *Zh.Fiz.Doslidzhen'*, **2**, 62 (1998).
13. A.E.Aliev, Ya.V.Burak, I.T.Lyseiko, *Izv. AN SSSR. Neorgan. Mater.*, **26**, 1991 (1990).
14. J.K.Srivastava, S.J.Supe, *J.Phys. D:Appl. Phys.*, **22**, 1537 (1989).
15. O.A.Kondakova, S.A.Dembovskij, A.S.Ziubin, *Fiz.Khim.Stekla*, **25**, 582 (1999).
16. S.Uda, R.Komatsu, K.Takayama, *J.Cryst. Growth*, **171**, 458 (1997).
17. M.Ignatovych, V.Holovey, A.Watterich et al., In: Physical Aspects of Luminescence of Complex Oxide Dielectrics (LOD'2004), III Intern. Workshop, Abstracts Book, Kharkiv, Ukraine (2004), p.35.
18. S.M.Kaczmarek, D.Podgorska, M.Berkowski, Multivalence States of Mn and Yb Ions in $Li_2B_4O_7$ Single Crystals and Glasses (2004). http://info.ifpan.edu.pl/pfi/abs/contrib/kaczmarek2.pdf
19. B.K.Vainstein, V.M.Fridkin, V.L.Indenbom, Modern Crystallography, Nauka, Moscow, (1979) [in Russian].
20. A.E.Aliev, I.N.Kholmanov, P.K.Khabibullaev, *Solid State Ionics*, **118**, 111 (1999).

Залежність термостимульованої люмінесценції монокристалів $Li_2B_4O_7$:Mn від концентрації домішки

В.М.Головей, В.І.Лямаєв, М.М.Біров, П.П.Пуга, А.М.Соломон

Одержано серію монокристалів $Li_2B_4O_7$:Mn з різною концентрацією легуючої домішки та досліджено їх термостимульовану люмінесценцію (ТСЛ). Форма кривих термовисвічування (КТВ) суттєво змінюється при підвищенні концентрації Mn, але на всіх них можна виділити два складні максимуми. Результати застосування метода часткового висвічування світлосуми вказують на наявність двох груп пасток, кожна з яких містить декілька рівнів прилипання з близькими величинами енергії активації. Залежність форми КТВ від поглинутої дози свідчить про перший порядок кінетики ТСЛ.